

## Technical Note

# Relaxation Times of Breast Tissue at 1.5T and 3T Measured Using IDEAL

Rebecca Rakow-Penner, MS, Bruce Daniel, MD, Huanzhou Yu, MS, Anne Sawyer-Glover, BS, RT, and Gary H. Glover, PhD\*

**Purpose:** To accurately measure T1 and T2 of breast fibroglandular tissue and fat at 1.5T and 3T, and note the partial volume effects of the admixture of fibroglandular tissue and fat on the relaxation rates using an approach termed iterative decomposition of water and fat with echo asymmetry and least squares estimation (IDEAL) imaging.

**Materials and Methods:** T1 and T2 values were measured on the right breasts of five healthy women at 1.5T and 3T. T1 data were collected using two sequences: inversion recovery without IDEAL, and inversion recovery with IDEAL. T2 data were collected using Hahn Echo scans. SNR and CNR analyses were conducted on collected data.

**Results:** T1 increased for both fat (21%) and glandular tissue (17%) from 1.5T to 3T. Thus, the TR and TI of breast protocols at 3T should be lengthened accordingly. SNR more than doubled for both tissue types from 1.5T to 3T. IDEAL imaging demonstrated the partial volume effects of fat and glandular tissue on measuring relaxation rates of independent tissue types.

**Conclusion:** With separated fat and water images, more precise measurements can be made for the lipid component in fat, and the water component in fibroglandular tissue.

**Key Words:** relaxation times; breast; MRI; IDEAL; fat/water  
**J. Magn. Reson. Imaging 2006;23:87–91.**  
 © 2005 Wiley-Liss, Inc.

THE HIGHER SENSITIVITY of magnetic resonance imaging (MRI) compared to x-ray mammography has led to growing clinical interest in the use of contrast-enhanced MRI of breast tissue, especially for women at high risk for breast cancer (1). Dynamic breast MRI depends on the sensitivity and specificity of the imaging protocol used, specifically the temporal and spatial resolution (2–4). With an increased signal-to-noise ratio

(SNR), the resultant higher spatial resolution and faster acquisition times may improve sensitivity and specificity for morphologic and dynamic breast MRI techniques. Doubling the field strength, such as imaging at 3T vs. 1.5T, approximately doubles the SNR, albeit at an increase in T1 (5). Imaging at 3T thus holds valuable potential for refining diagnostic breast MRI.

In transitioning breast imaging protocols from 1.5T to 3T, the scan parameters should be adapted to optimize contrast and SNR at the increased field strength. Generally, higher field strength increases the longitudinal relaxation time (T1) and slightly decreases the transverse relaxation time (T2) of breast tissues (6). In defining a scan protocol for a tissue of interest, the relaxation time (TR) should increase as T1 increases; otherwise, magnetization saturation effects will diminish the SNR gain (7,8). Thus the TR should be adjusted according to the T1 for the tissue of interest. Breast tissue is primarily composed of glandular tissue and lipids. To the best of our knowledge, there are currently no published values for T1 and T2 of breast glandular tissue and fat at 3T. However, subcutaneous fat has been measured (9) and provides a guiding value for breast fat T1 and T2 relaxation times.

Relaxation times for breast tissue have been measured at field strengths of  $\leq 1.5T$  (10–14). The published values often contradict one another, possibly because of inconsistent methods, differences in equipment, and varying admixtures of fat and water in breast tissue. The relaxation rates of other human tissues, such as musculoskeletal tissue (15), abdominal and pelvic tissue (9), and brain (16), have been measured at 3T. These studies indicated that the SNR and T1 of the respective measured tissues increased from 1.5T to 3T. They also noted a minimal change of T2 with increasing field strength.

In the present study we measured the T1 and T2 values of breast fibroglandular tissue and fat at 1.5T and 3T, and performed a contrast-to-noise ratio (CNR) analysis of breast imaging. Importantly, this study notes the partial volume effects of the admixture of fat and glandular tissue in breasts when the independent relaxation rates of the respective tissues are measured. These partial volume effects result from the biological water component in fat, and the lipid component in glandular tissue, as well as breast architecture. To

Department of Radiology, School of Medicine, Stanford University, Stanford, California, USA.

Contract grant sponsor: National Institutes of Health (NIH); Contract grant number: P41-RR09784.

\*Address reprint requests to: G.H.G., Stanford University School of Medicine, Lucas MR Center, 1201 Welch Road, Stanford, CA 94305-5488. E-mail: garyglover@stanford.edu.

Received January 3, 2005; Accepted September 27, 2005.

DOI 10.1002/jmri.20469

Published online 28 November 2005 in Wiley InterScience (www.interscience.wiley.com).

eliminate these effects we used an approach termed iterative decomposition of water and fat with echo asymmetry and least squares estimation (IDEAL) (17,18), which provides separated fat and water images on which to base the T1 and T2 measurements. IDEAL uses three measurements with different TEs to separate fat and water. It is robust to B0 inhomogeneities, since a map of the field strength is calculated as part of the reconstruction (18).

## MATERIALS AND METHODS

Five healthy women, ranging in age between 24 and 51 years (mean age = 36.4 years, standard deviation (SD) = 12.6), participated in this study after they gave informed consent according to a protocol approved by the local IRB. The study consisted of three scan sequences performed on the right breast of each volunteer at 1.5T and 3T (Echospeed whole-body magnet; GE Healthcare, Waukesha, WI, USA): 1) T1 data collection using fast spin-echo inversion recovery (FSE-IR) for combined fat and water images, 2) T2 data collection using Hahn echo acquisition, and 3) T1 data collection using FSE-IR IDEAL for separated fat and water images. The FSE-IR IDEAL technique provides a combined image as well. However, the IDEAL combined image results in a lower SNR than its separated fat and water images, and thus was not used for any calculations. The SNR of the combined image is diminished because of correlation between the fat and water images (20). A non-IDEAL FSE-IR was used to measure a combined fat and water image. Note that there is some bias toward the IDEAL separated images with regard to SNR because the reconstructions are an outcome of three excitations, whereas the non-IDEAL image is an outcome of one excitation. The FSE-IR and Hahn sequences are commercially available. The FSE-IR IDEAL sequence is an in-house-developed sequence. This technique was preferred for T1 measurements over other, faster techniques because of its robustness and dependability. Since the volunteers were all healthy and no contrast was injected, time was not a limiting factor. If one wanted to perform T1 measurements on patients or a large population, a faster but potentially less reliable technique might be preferable.

Four-channel receive-only breast coils (Invivo/MRI Devices Corp., Waukesha, WI, USA) were used to acquire the data. Each volunteer was scanned at both field strengths no more than 2 days apart to control for menstrual cycle variations in the breast tissue within (but not among) individuals.

### FSE-IR Scans

The FSE-IR protocol for T1 measurements consisted of four scans with variable TIs of 3000, 800, 300, and 150 msec, and the following parameters: TE = 18.5 msec, TR = 4000 msec, echo train length = 8, bandwidth = 15.63 kHz, FOV = 20 mm × 20 mm, slice thickness = 5 mm, slice direction = sagittal, NEX = 1, resolution = 256 × 128. An adiabatic inversion pulse was used in the vendor-supplied pulse sequence. Only four TIs were collected, due to time

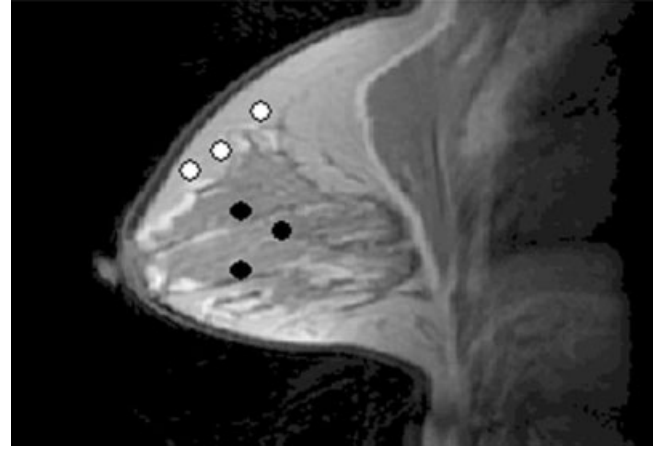


**Figure 1.** The white dots represent sample fat ROIs, and the black dots represent sample glandular-tissue ROIs on an IDEAL combined image.

constraints. To calculate T1, we assumed monoexponential decay. The following equation was solved for T1, given the measurements  $M_i$  corresponding to the four TIs:

$$M_i = M_0[1 - 2(1 + \epsilon)\exp(-T_i/T_1)], \quad (1)$$

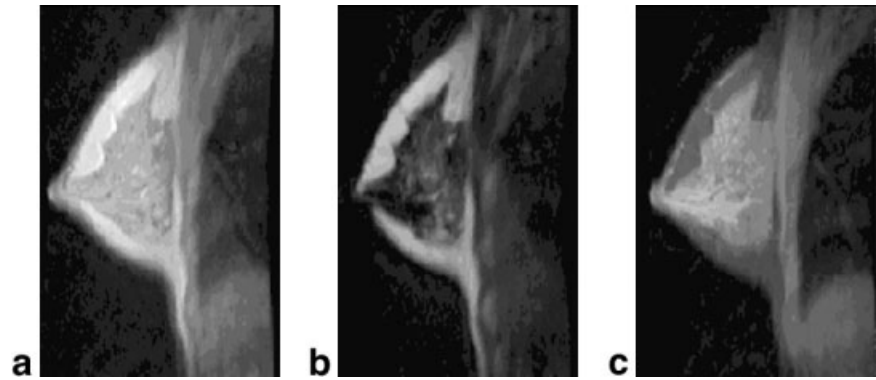
where  $M_0$  is the equilibrium magnetization level, and  $\epsilon$  is an error term that accounts for imperfect magnetization inversion by the 180° pulse ( $\epsilon$  was nominally close to zero, but no matter how small it was it remained in the calculation). The equation was solved using the Nelder-Mead simplex method as implemented by MATLAB (Natick, MA, USA). When the T1 for fat was calculated, the received signal,  $M$ , resulted from an average of three regions of interest (ROIs) drawn in the fat region for each TI value per volunteer (see Fig. 1). The size of the ROIs varied because they were drawn to maximize a region of homogeneous tissue type. After each volunteer's T1 value in fat was solved for, the final value resulted from averaging T1 values across all volunteers for a given field strength. The same method was used to calculate the T1 of glandular tissue. The order of averaging the signals and then estimating the parameters per volunteer vs. estimating the parameters per volunteer and then averaging the parameters did not produce significantly different results.

### T2 scans

The protocol for the T2 scans consisted of two Hahn echo scans with two TEs (TE1 and TE2) of 20 and 100 msec, respectively, and the following scan parameters: TR = 2000 msec, bandwidth of 15.63, FOV = 20 mm, slice thickness = 5 mm, slice direction = sagittal, NEX = 1, resolution = 256 × 128. Assuming a monoexponential T2 decay, the transverse magnetization  $M_i$  for TE<sub>i</sub> is given by:

$$M_i = M_0(\exp(-TE_i/T_2)), \quad (2)$$

**Figure 2.** IDEAL images at 1.5T with a T1 of 3000 msec: (a) combined fat and water, (b) fat, and (c) water. Note that the water component of the fatty tissue is visible in slice c.



where  $M_0$  is a constant. T2 and  $M_0$  can be solved with the two known measurements  $M_i(TE_i)$ . We measured  $M$  for fat and glandular tissue by placing three ROIs in the fat and glandular-tissue regions, respectively, of the reconstructed image. The fat and water ROIs were averaged independently per volunteer. As in the T1 calculation, the overall T2 values for each fat and water ROI resulted from an average across volunteers per field strength.

### IDEAL

The parameters of the IDEAL sequence remained the same as for the non-IDEAL FSE-IR protocol. The IDEAL technique produces three sets of images: combined fat and water, separated water, and separated fat (18) (see Fig. 2). Because of the above-mentioned SNR disadvantage, we did not use the IDEAL combined image. For the separated images, ROIs outside of the fat regions in the fat images, and outside glandular-tissue regions in the water images were not measured because it proved difficult to draw an ROI of fat in water and vice versa consistently across volunteers. Thus, only three ROIs were drawn in each separated image in the specified tissue type. As in the non-IDEAL analysis, the size of the ROIs depended on a maximized area of the homogeneous tissue of interest. The ROIs drawn in the IDEAL and non-IDEAL analyses differed slightly because the acquisitions differed, although the ROIs in both acquisitions were approximately in the same position and of the same size. The calculation process followed the previous approach of solving T1 for each volunteer in the separated fat and water images, and then averaging over all the volunteers.

SNR and CNR calculations were performed on the FSE-IR T1 data. The signal was taken to be the average  $M_0$  values (fully relaxed magnetization) in the two tissue types for each subject at each field. The noise was measured with an ROI placed in the  $M_0$  image corner, with care taken to avoid ghosting artifacts. No correction was made for the Rician distribution of the magnitude images. CNR measurements were obtained between fat and water using three specified ROIs (fat, glandular tissue, and noise) placed in FSE-IR images at each of the four T1s.

### RESULTS

Increasing field strength led to an increase in T1 values for both fat and water (refer to Table 1). The SD analysis was performed between subjects. IDEAL imaging provided lower values for T1 in fat, and higher values for T1 in water at both 1.5T and 3T. Significant differences between T1 values were examined with t-tests for fat non-IDEAL and IDEAL at 1.5T, water non-IDEAL and IDEAL at 1.5T, fat non-IDEAL and IDEAL at 3T, and water non-IDEAL and IDEAL at 3T (Table 1). These significant  $P$ -values demonstrate a trend in the impact of the admixture of fat and water in both fatty and fibroglandular tissue. Note that the SDs for the IDEAL technique are smaller than those for the non-IDEAL approach. This may partially result from the bias of the 3 NEX IDEAL vs. the 1 NEX non-IDEAL.

T2 values (refer to Table 2) did not demonstrate a significant difference between field strengths of either tissue. Also, T2 values did not significantly differ between tissue types at either field strength. Since these

Table 1  
T1 Relaxation Times at 1.5T and 3T†

	Breast tissue	1.5T		3T	
		T1 (average $\pm$ SD, msec)	SNR (average)	T1 (average $\pm$ SD, msec)	SNR (average)
FSE-IR non-IDEAL	Fat	372.04 $\pm$ 8.6	97	449.27 $\pm$ 26.09**	203
	Glandular	1135.98 $\pm$ 151.37	67	1324.42 $\pm$ 167.63**	138
FSE-IR with IDEAL	Fat	296.01 $\pm$ 12.94*	118	366.78 $\pm$ 7.75**	274
	Glandular	1266.18 $\pm$ 81.8*	96	1444.83 $\pm$ 92.7**	202

†The standard deviation listed is for the deviation between T1 values.

\* $P \leq 0.05$  between non-IDEAL vs. IDEAL with the same field strength.

\*\* $P \leq 0.05$  between 1.5T and 3T of the same tissue type and scan parameters.

Table 2  
T2 Relaxation Times at 1.5T and 3T\*

Breast tissue	1.5T		3T	
	T2 (msec)	SD	T2 (msec)	SD
Fat	53.33	2.11	52.96	1.54
Glandular	57.51	10.15	54.36	9.35

\*There was no significant difference between T2 values due to tissue types or field strength.

results showed little difference, IDEAL results were not measured.

The ratio of the fat/water CNR values at 3T and 1.5T without IDEAL was 2.18. The CNR ratio between 3T and 1.5T with IDEAL was 3.15.

## DISCUSSION

The results indicate that with increasing field strength, from 1.5T to 3T the T1s of fat and fibroglandular tissue increased by 21% and 17%, respectively, using the non-IDEAL technique. With IDEAL imaging the T1s of fat and fibroglandular tissue increased by 23% and 14%, respectively. The parameters used for scanning at 3T must be optimized accordingly. In particular, TR and TI values should be lengthened at 3T. According to Edelstein et al (19), the TR for saturation recovery imaging, and the TI for inversion recovery imaging should be set approximately equal to the T1 of the tissue of interest at a given field strength.

Our novel approach for measuring T1 of fat and glandular tissues from IDEAL separated images provides greater precision in T1 measurements by reducing partial volume effects. For measurements of the lipid component of fat or the water component of glandular tissue, optimizing scan protocols based on values obtained from IDEAL T1 images will provide more exact results. When the combined IDEAL image results (Fig. 2a) are compared with the IDEAL image results in which fat and water are separated (Fig. 2b and c), the fat T1 values across field strengths drop notably. This is because breast fat has both water and lipid components. The values measured in the IDEAL separated fat image provide only the T1 values of the lipid component. Thus, to accurately measure the T1 of the lipid component in breast tissue, IDEAL separation is recommended. On the other hand, T1s of fibroglandular tissue in the IDEAL water separated images are significantly higher than in the combined measurements, indicating the value of separating the water and lipid components when examining the water content in breast tissue.

T2, as measured with a spin-echo sequence, does not significantly vary between 1.5T and 3T (it varies less than 5 msec), nor does it vary significantly between fat and glandular tissue. Thus the TE does not require modification.

A SNR analysis demonstrated the predictable linear upward relationship between SNR and field strength. CNR calculations confirmed that T1 tissue contrast improves with increasing field strength. This en-

hancement more than compensates for any loss in saturation recovery due to higher magnetic fields. This paper focused on the SNR and CNR of fat and glandular tissue without contrast agents. For diagnostic purposes, measuring these ratios with contrast agents would be useful and may be done in future studies.

The results of this study can serve as a guideline for adjusting breast protocols for 3T imaging, and specifically indicate that the TR must be lengthened proportionally to the T1 of the breast tissue of interest. Our study had the following limitations: 1) a small sample size was used, 2) data were collected from healthy volunteers vs. cancer patients, and 3) menstrual variations were controlled for within but not among the volunteers. The results from our limited sample group provide general protocol guidelines for glandular and fat tissue. A larger sample group may provide more statistically accurate results. Because of the length of the scans and the repetition of acquisitions at two field strengths, data were collected on healthy volunteers rather than cancer patients. T1 data on lesions are useful and may be included in future studies. Our study controlled for menstrual variations within volunteers by scanning them at both field strengths within a short span of time. Controlling for menstrual variations among volunteers would have required greater flexibility of magnet time, and inconvenienced the volunteers.

In conclusion, T1 measurements in the breast with IDEAL imaging provide more precise values for fat and glandular tissue, and reduce patient-to-patient variability in the values measured. The TRs and TIs of breast protocols at 3T must be lengthened from the values used at 1.5T to account for the increase in T1 of breast tissue.

## ACKNOWLEDGMENTS

We thank Drs. Kim Butts and Karl Vigen for their input on this project, and Ann Shimakawa and Dr. Scott Reeder for providing the FSE-IR IDEAL sequence.

## REFERENCES

1. Kriege M, Brekelmans C, Boetes C, et al. Efficacy of MRI and mammography for breast-cancer screening in women with a familial or genetic predisposition. *N Engl J Med* 2004;351:427-437.
2. Agoston AT, Daniel BL, Herfkens RJ, et al. Intensity-modulated parametric mapping for simultaneous display of rapid dynamic and high-spatial-resolution breast MR imaging data. *Radiographics* 2001;21:217-226.
3. Kuhl CK, Bieling HB, Gieseke J, et al. Healthy premenopausal breast parenchyma in dynamic contrast-enhanced MR imaging of the breast: normal contrast medium enhancement and cyclical-phase dependency. *Radiology* 1997;203:137-144.
4. Song HK, Dougherty L, Schnall MD. Simultaneous acquisition of multiple resolution images for dynamic contrast enhanced imaging of the breast. *Magn Reson Med* 2001;46:503-509.
5. Haacke EM, Brown RW, Thompson MR, et al. *Magnetic resonance imaging: physical principles and sequence design*. New York: John Wiley and Sons; 1999. p 1-914.

6. Bottomley PA, Foster TH, Argersinger RE, et al. A review of normal tissue hydrogen NMR relaxation times and relaxation mechanisms from 1–100 MHz: dependence on tissue type, NMR frequency, temperatures, species, excision and age. *Med Phys* 1984;11:425–448.
7. Jezzard P, Diewell S, Balaband RS. MR relaxation times in human brain: measurement at 4T. *Radiology* 1996;199:773–779.
8. Crooks LE, Arakawa M, Hoenninger J, et al. Magnetic resonance imaging: effects of magnetic field strength. *Radiology* 1984;151:127–133.
9. de Bazelaire CMJ, Duhamel GD, Rofsky NM, et al. MR imaging relaxation times of abdominal and pelvic tissues measured in vivo at 3.0T: preliminary results. *Radiology* 2004;230:652–659.
10. Bottomley PA, Hardy CJ, Argersinger RE, et al. A review of H nuclear magnetic resonance relaxation in pathology: are T1 and T2 diagnostic? *Med Phys* 1987;14:1–37.
11. Heywang SH, Fenzl G, Hah Dietbert, et al. MR imaging of the breast: comparison with mammography and ultrasound. *J Comput Assist Tomogr* 1986;10:615–620.
12. Partain CL, Kulkarni MV, Price RR, et al. Magnetic resonance imaging of the breast: functional T1 and three-dimensional imaging. *Cardiovasc Intervent Radiol* 1986;8:292–299.
13. El Yousef SJ, O'Connell DM, Duchesneau RH, et al. Benign and malignant breast disease: magnetic resonance and radiofrequency pulse sequences. *AJR Am J Roentgenol* 1985;145:1–8.
14. Merchant TE, Thelissen GRP, de Graaf PW, et al. Application of a mixed imaging sequence for MR imaging characterization of human breast disease. *Acta Radiol* 1993;34:356–361.
15. Gold GE, Han E, Stainsby J, et al. Musculoskeletal MRI at 3.0T: relaxation times and image contrast. *AJR Am J Roentgenol* 2004;183:343–351.
16. Wansapura JP, Holland SK, Dunn RS, et al. NMR relaxation times in the human brain at 3.0 Tesla. *J Magn Reson Imaging* 1999;9:531–538.
17. Glover GH, Schneider E. Three-point Dixon technique for true water/fat decomposition of B0 inhomogeneity correction. *Magn Reson Med* 1991;18:371–383.
18. Reeder SB, Pineda AR, Wen Z, et al. Iterative decomposition of water and fat with echo asymmetry and least squares estimation (IDEAL): application with fast spin-echo imaging. *Magn Reson Med* 2005;54:636–644.
19. Edelstein WA, Bottomley PA, Hart HR, et al. Signal, noise, and contrast in nuclear magnetic resonance (NMR) imaging. *J Comput Assist Tomogr* 1983;7:391–401.
20. Yu H, Reeder SB, Shimakawa A, Gold GE, Pelc NJ, Brittain JH. Implementation and noise analysis of chemical shift correction for fast spin echo Dixon imaging. In: *Proceedings of the 12th Annual Meeting of ISMRM, Kyoto, Japan, 2004.* p 2686.